Aligned Growth of Gold Nanorods in PMMA Channels: Parallel Preparation of Nanogaps

Titoo Jain,[†] Samuel Lara-Avila,[‡] Yann-Vai Kervennic,[‡] Kasper Moth-Poulsen,[§] Kasper Nørgaard,[†] Sergey Kubatkin,[‡,*] and Thomas Bjørnholm[†,*]

[†]Nano-Science Center and Department of Chemistry, University of Copenhagen, Universitetsparken 5, DK-2100, Copenhagen Ø, Denmark, and [‡]Department of Microtechnology and Nanoscience and [§]Department of Chemical and Biological Engineering, Chalmers University of Technology, Kemivägen 9, S-41296 Gothenburg, Sweden

ABSTRACT

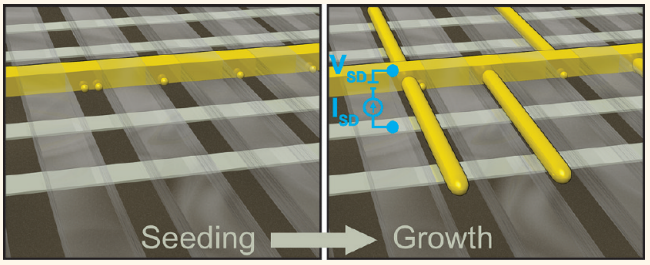

We demonstrate alignment and positional control of gold nanorods grown *in situ* on substrates using a seed-mediated synthetic approach. Alignment control is obtained by directing the growth of spherical nanoparticle seeds into nanorods in well-defined poly(methyl methacrylate) nanochannels. Substrates with prepatterned metallic electrodes provide an additional handle for the position of the gold nanorods and yield nanometer-sized gaps between the electrode and nanorod. The presented approach is a novel demonstration of bottom-up device fabrication of multiple nanogap junctions on a single chip mediated *via in situ* growth of gold nanorods acting as nanoelectrodes.

KEYWORDS: gold nanorods · nanoparticles · nanogaps · self-assembly · single-molecule electronics · nanoelectrodes · junctions

The fabrication of metallic electrode pairs separated by a few nanometers is a fundamental challenge in nanotechnology and is well beyond the capabilities of current microfabrication techniques.[1] Possible areas of application lie within, for example, single-molecule electronics,[2] spectroscopy,[3] and plasmonics.[4] Thus far, top-down approaches such as the mechanical controllable break junction,[5,6] shadow mask evaporation,[7] and electromigration[8,9] have proven successful in fabricating nanoelectrodes. Common shortcomings of these techniques are time consumption, low throughput, and the requirement for expensive and complicated experimental setups normally operating at cryogenic temperatures.[10]

In contrast, bottom-up approaches for the fabrication of nanogap devices are currently much less explored, despite their potential for being more cost-effective and providing parallel fabrication routes for the production of multiple devices in only a few synthetic steps.[11−14] Efforts in this direction have typically focused on the integration of (bottom-up) prepared nanoparticles into devices, where precise control of placement is required.[15−18]

Gold nanorods (AuNRs) have received considerable attention due to their facile synthesis and interesting physical properties, many of which originate from their anisotropic nature. Using a variety of methods, AuNRs have been self-assembled in one,[19,20] two,[21] and three[22] dimensions. Directional assembly of AuNRs has been obtained *via* electric field-assisted deposition between lithographically defined electrodes,[23] using carbon nanotubes as templates,[24] stretching AuNR-embedded poly(vinyl alcohol) polymer films,[25,26] and employing capillary forces in polymer guiding templates.[27,28] Similar strategies have been employed for ~5 μm long gold nanowires over large areas,[29] and nanowires of different materials have been assembled using, for example, flow-induced alignment,[30] while fabrication of carbon nanotube arrays[31] has been demonstrated in scalable high-performance electronics.[32]

Herein, we employ a combination of top-down and bottom-up approaches for the fabrication of nanogap junctions by directed *in situ* growth of AuNR-based nanostructures inside prepatterned poly(methyl methacrylate) (PMMA) nanochannels on silicon dioxide surfaces. The effect of PMMA channel width on AuNR alignment

* Address correspondence to sergey.kubatkin@chalmers.se, thob@adm.ku.dk.

Received for review December 20, 2011 and accepted April 11, 2012.

Published online April 11, 2012
10.1021/nn204986y

© 2012 American Chemical Society

is examined, and we show how the introduction of prepatterned metallic electrodes on the substrate can be used not only to control the AuNR position but also to enable electronic characterization of the interface between AuNRs and the lithographically defined electrodes. At this interface, we found the presence of nanogaps, formed upon seed-mediated growth of AuNRs; ligand-stabilized gold nanoparticle seeds assemble preferentially close to the prepatterned electrodes, and growth of the seed particles into AuNRs primarily happens in a direction away from the prepatterned electrodes, resulting in nanogaps at the interface.

This study demonstrate control over position and orientation of AuNRs grown directly on substrates using a seed-mediated growth approach and may contribute to the further development of parallel fabrication schemes for nanogap electronics.

RESULTS AND DISCUSSION

Directional Growth of AuNRs in PMMA Channels. The growth of AuNRs is based on a seed-mediated approach to prepare anisotropic gold nanoparticles.[33] The synthesis is readily performed in aqueous solutions of cetyltrimethylammonium bromide (CTAB) and results in fairly monodisperse CTAB-capped AuNRs after purification (see Supporting Information, Figure S1).

Taub *et al.*[34] and later Zamborini *et al.*[35,36] studied the growth of AuNRs directly on surfaces from seed precursors. In these studies, the orientation and position of the resulting AuNRs are not well controlled, and a large fraction of non-rod-shaped byproduct is observed in the growth process. Some control of position was shown using soft lithography to print micrometer wide tracks of the nanoparticle seeds on the substrate followed by growth, but the yield of AuNRs was low, and no directional control was obtained.[37] Locally aligned AuNRs have been obtained through a surface chemical amidation reaction; however, no explanation for the alignment has yet been presented.[38]

In the present work, thermally oxidized silicon chips were coated with the positive resist PMMA and nanochannels were patterned by electron beam lithography; the exposed and developed areas were removed, uncovering the silicon oxide surface. AuNRs were synthesized directly on the substrate from seed precursors, as illustrated schematically in Figure 1A.

CTAB-stabilized gold nanoparticle seeds were deposited on the substrate by immersion, and the seeded substrate was placed into a growth solution that promotes unidirectional growth of AuNRs, with lengths up to hundreds of nanometers (details of the synthesis steps are given in the Experimental Section). Figure 1B shows a scanning electron microscopy (SEM) image after growth of AuNRs in predefined PMMA channels. The widths, w, of the channels were varied between

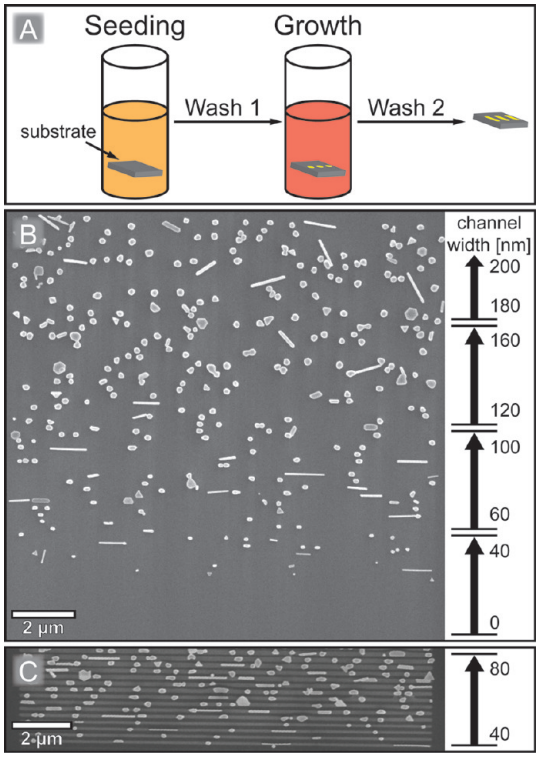

Figure 1. (A) Schematic illustration of the *in situ* growth of AuNRs on a 1 × 1 cm^2 Si/SiO$_2$ substrate. (B) SEM image of AuNRs grown in 20−200 nm wide PMMA channels. (C) Image of highly aligned AuNRs in 40−80 nm wide channels showing the templating effect of the PMMA nanochannels.

$20 \leq w \leq 200$ nm in increments of 20 nm. Growth results in parallel alignment of rods in narrow channels with widths of $20 \leq w \leq 80$ nm (Figure 1B), but for channels with $w > 100$ nm, a less strict confinement causes the AuNRs to be less aligned. Figure 1C shows the channels templating the direction of AuNRs. The presence of non-rod-shaped byproduct is common in seed-mediated preparations of AuNRs, and a large fraction of spherical particles are also present here. It is well-established that only a small percentage of the seeds actually evolve into nanorods.[36,39] In solution-based synthesis of AuNRs, the majority of byproduct can typically be removed by centrifugation purification,[40] a process that is not possible on a substrate. The nanorods remain aligned on the surface after removal (lift-off) of PMMA in acetone.

Aligned Growth from Prepatterned Metallic Contacts. The integration of AuNRs into electronically addressable nanogap devices requires, in addition to directional and positional control, a means for electronic addressability of the nanorods. For this aim, submicrometer metallic electrodes were fabricated by e-beam lithography on an oxidized silicon substrate (see Experimental Section). PMMA channels were used to direct the growth of AuNRs perpendicular to the prepatterned metallic electrodes, as illustrated in Figure 2A−D.

The chip design consists of five parallel electrodes: one thick central gold electrode and two thin chromium electrodes on either side (see Experimental Section for

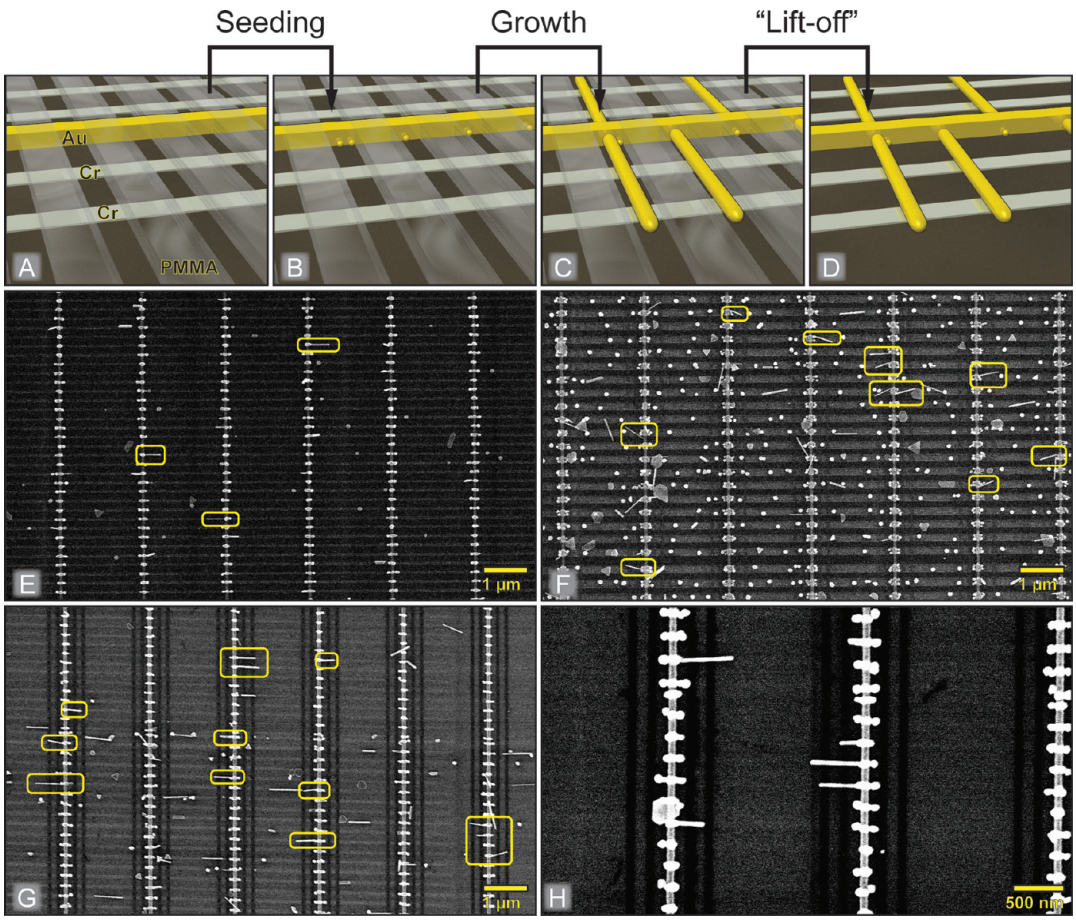

Figure 2. Aligned growth of AuNRs from prepatterened metallic contacts. (A) Schematic illustration of a prepatterned chip with four parallel Cr electrodes surrounding a Au electrode and PMMA channels positioned perpendicular to the metal wires. (B–D) Seeding step followed by growth of AuNRs and removal of PMMA. (E) SEM images of the chip before lift-off in acetone of $w = 40$ nm and (F) $w = 140$ nm wide channels. (G) Image after lift-off in acetone at the area with channel widths of $w = 20$ and $w = 40$ nm, and (H) a close-up clearly showing AuNRs grown perpendicularly from the Au electrode bridging the two Cr electrodes. Yellow markers highlight AuNRs that originate from a Au wire and touch or bridge both Cr wires.

details), enabling two- or four-terminal measurements. All metallic electrodes are completely coated with PMMA, and nanochannels with widths varying between $20 \leq w \leq 200$ nm are defined across the electrodes so that the silicon oxide surface and the metallic electrodes become accessible to seed-mediated growth of AuNRs. We observed that the seeds assemble preferentially inside the PMMA channels and particularly near the gold electrode (see Supporting Information). We attribute this finding to a combination of the hydrophilic/hydrophobic interface found in the nanochannels and capillary forces; similar observations on assembly of nanoparticles in nanochannels have been studied in detail by others.[27,29,41] After exposing the chips to a growth solution, the AuNRs grow in close proximity to the gold electrodes, as shown in SEM images (Figure 2E–H). For narrow channels ($w = 40$ nm, Figure 2E) and wide channels ($w = 140$ nm, Figure 2F), the AuNRs protrude from the Au electrode bridging the two adjacent Cr electrodes (which are not clearly visible due to charging effects caused by the insulating PMMA layer). After removal of PMMA, the parallel Cr electrodes are visible as dark vertical lines and the AuNRs remain present on the SiO_2 surface (Figure 2G, $w = 20$ and 40 nm). Figure 2H displays a close-up view of four AuNRs that have grown perpendicular to the Au electrode, while bridging both Cr electrodes. Given the geometry of the chip, the prepatterned chromium electrodes can restrict the growth of AuNRs and not all of the AuNRs will grow to fully bridge all contacts. More images before and after lift-off in acetone are presented in the Supporting Information (Figures S2 and S3, respectively). The PMMA channels confine and direct the growth of the AuNRs. Nanorods in wider channels have freedom to grow in different directions, while AuNRs in narrow channels are simultaneously restricted and guided by the walls of PMMA. Table 1 shows that the average orientation angle and angle distribution (with respect to the channel direction, see Figure S5) increase with the width of the channels and confirms that the PMMA channels play a crucial role in guiding the growth of AuNRs on the substrate. Growing the AuNRs on prepatterned substrates without the PMMA nanochannels results in

randomly aligned AuNRs in the space between metal electrodes (Supporting Information, Figure S4).

The average dimensions of the AuNRs are 453 ± 114 nm in length and 37 ± 10 nm in width. The dimensions do not vary significantly with channel width, although the diameter of the AuNRs is confined in w = 20 nm wide channels. Thus, for channels w > 20 nm, AuNR growth in the transversal direction is terminated before encountering the channel walls. The AuNR dimensions are similar to those obtained elsewhere for growth on surfaces.[35,37] The yield of AuNRs (*i.e.*, ratio between the number of rod-shaped and the total number of particles) is ~5−10% regardless of the channel width. A low AuNR yield is expected when using the seed-mediated growth approach directly on surfaces[34−36] and even in solution.[39] The most widely accepted explanation for the AuNR growth mechanism in solution suggests that AuNRs evolve along one axis due to preferential binding of CTAB bilayers to specific crystallographic facets ({100} and {110}) of the developing seeds.[39] On a 2D surface, one could speculate that many seed particles will have the facets preferred by CTAB oriented in such a way that their growth direction is restricted. Assembling the seed particles with their facets oriented favorably with respect to growth could significantly increase the AuNR to by-product ratio. Such orientation could be achieved by utilizing molecular linkers (*e.g.*, dithiols) to facilitate oriented self-assembly of the seed particles preceding growth. Table 1 shows that a large fraction, n_2 probe ~60−89%, of the grown AuNRs are bridging at least one Cr electrode, allowing for two-probe measurements, while n_4 probe ~19−47% allows for four-probe measurements because the AuNRs bridge both Cr electrodes. The probability of finding AuNRs connected to prepatterned gold electrodes is greater than finding them anywhere else on the substrate (Supporting Information, Table S1), emphasizing that gold nanoparticle seeds preferentially assemble and grow close to the prepatterned gold electrodes. These numbers are derived from the yields of AuNRs in a given configuration within a small area (see Supporting Information, Table S1, and accompanying discussion for details). Despite the moderate yields, the present method is scalable to wafer-sized substrates and would potentially allow for thousands of nanogaps in a few synthesis steps after microfabrication of the underlying electrode patterns.

Pregrown AuNRs do not assemble in the PMMA channels, proving that the above observations are indeed due to *in situ* growth (Supporting Information, Figure S6).

Nanogap Characterization. We found that nanogaps of 1−5 nm form at the interface between *in situ* grown AuNRs and the prepatterned Au electrode, as demonstrated by transmission electron microscopy (TEM) and electrical characterization. Gold electrodes were fabricated on 100 nm thick silicon nitride membranes suitable for TEM characterization (Figure 3A). The AuNRs were grown using the seed-mediated approach without PMMA nanochannels.

TABLE 1. Angle Distribution and Possible Device Yield of AuNRs Grown on Prepatterned Electrodes

channel width (nm)	angle[a] (deg)	n_4 probe[b] (%)	n_2 probe[b] (%)
20	5.1 ± 8.9	18.9	59.5
40	5.8 ± 11.8	18.8	78.3
60	13.0 ± 19.7	46.5	74.4
80	23.3 ± 22.7	43.3	80.0
120	21.0 ± 21.5	38.5	78.5
140	24.1 ± 20.4	31.8	84.9
160	25.1 ± 22.1	32.4	81.1
180	28.9 ± 26.7	7.4	88.9
200	29.3 ± 23.3	18.3	73.9

[a] Average orientation angle with respect to the channel direction. The alignment angle is defined schematically in Supporting Information Figure S5. [b] Fraction of electronically addressable AuNRs in a four- or two-terminal configuration; n_4 probe is a subset of n_2 probe (see Supporting Information Table S1 for details).

TEM imaging of the nitride membranes was carried out before and after exposure of the chips to seed and growth solutions. The preference for seed particles to assemble near the interface to the Au electrode is verified by imaging prior to growth (see Supporting Information Figure S7). Figure 3C,D reveals the presence of grown AuNRs mainly protruding from the Au wire. AuNRs tend to grow away from the main Au electrodes, an observation that is consistent with those reported elsewhere[36] that also suggest that Au seed particles are either inhibited by, or tend to grow in a direction away from, nearby objects. Figure 3E shows the interface between a lithographically defined gold wire and an *in situ* grown AuNR revealing a ~1 nm gap. Some junctions appear to be fused (Figure 3F) at the interface. Fused AuNR−AuNR junctions are not uncommon.[11] It is not possible for us to address if the fusing occurs due to a lack of stabilizing molecules in the nanogap or if it happens during the TEM imaging due to the high-energy electron beam exposing the gold during image acquisition. The TEM micrographs (Figure 3C−F) also show the microcrystalline structure of the lithographically prepared electrodes as well as the highly ordered, single-crystal AuNRs.

The formation of nanogaps was further confirmed through electrical characterization by exploiting the fact that the electrical resistance of a metallic contact is maximum $h/2e^2 \sim 12.9$ kΩ for a single Au atom,[42] while the (tunneling) resistance of a nanogap is typically much higher (MΩ to GΩ) and increases exponentially with its size x as ~exp(kx), where the decay constant k depends on the particular details of the interface between the electrodes. In order to enable electrical measurements, the device architecture was modified from that shown in Figure 2 and designed to ensure that only one AuNR junction is sampled with each

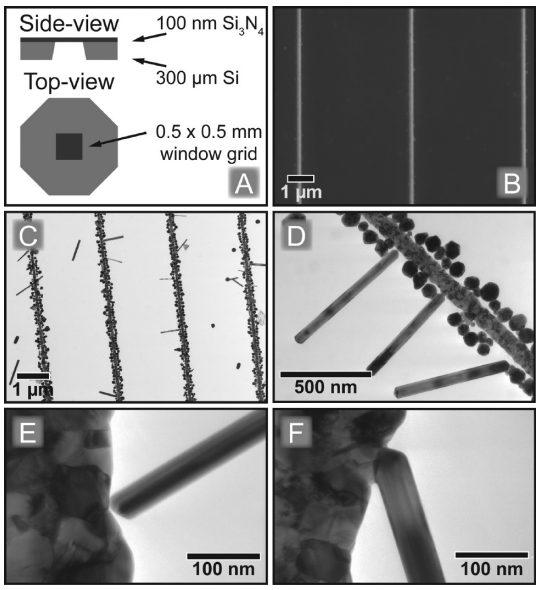

Figure 3. (A) Schematic illustration of the side and top view of a Si_3N_4 TEM membrane grid. (B) SEM image of e-beam defined Au wires. (C) TEM overview and (D) close-up subsequent to seeding and growth of AuNRs. Interface between Au wire and AuNR revealing the presence of (E) nanogaps and (F) fused junctions.

measurement (see Supporting Information Figure S8A). Measurements of the electrical resistance of AuNRs are performed at room temperature using the lateral chromium contacts (see Figure 4, inset); poor electrical contact between chromium and AuNRs is initially observed and can be attributed to the native oxide on chromium in contact with the organic CTAB bilayer at the surface of the AuNRs. The contact is improved by applying relatively high voltages (up to ~10 V) while limiting the current to a maximum of 1 μA. Once a good contact to the AuNR is established, the tunneling current from the AuNR into the central gold electrode is measured in a two- or four-probe configuration (for AuNR device images, see Supporting Information Figure S8B,C). Typical values of tunneling resistances are on the order of 1−10 GΩ, which is expected for a ~1 nm wide nanogap.[8]

The exact sizes of the nanogaps fabricated using this method vary (2.4 ± 1.5 nm, determined from TEM images). In future experiments, the gap may be tailored by assembling spacer molecules onto the Au electrode prior to seeding and growth. Not only would this allow for controlled gap sizes, but it would also lead to a better yield of AuNRs provided that the assembly would favor the orientation of the seed particles with respect to the

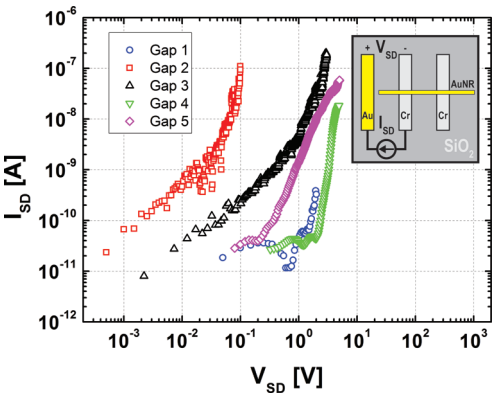

Figure 4. Electrical characterization of chemically fabricated nanogaps. The low-bias (tunneling) resistance of five different gaps formed between the AuNRs and the predefined Au central electrode, measured in a two- or four-probe configuration (inset), indicates a gap size of ~1 nm.

preferred crystal facets promoting growth. Potential applications of these nanogap junctions may be found in diverse fields as plasmonics,[4] single-molecule spectroscopy,[3] and for the creation of molecular junctions.[1] In preliminary experiments performed at our laboratories, a conjugated wire-like molecule was deposited from solution into the nanogap, resulting in a significant increase of the nanogap conductivity. Further studies of these molecular junctions are currently in progress.

CONCLUSIONS

We have demonstrated *in situ* growth of highly aligned AuNRs at predefined positions directly on surfaces. The position and direction of growth of the AuNRs was controlled *via* a combination of self-assembly of nanoparticle seeds and directed growth of AuNRs in PMMA nanochannels. Nanogaps were found at the interface between AuNRs and prepatterned metallic contacts, as confirmed by TEM imaging and electrical characterization.

This work demonstrates potential for bottom-up growth of electrically addressable devices, where top-down preparation of the metallic contacts prior to nanogap formation eliminates potential damage of the nanogap due to post-processing steps. Future work may involve the use of chemically grown nanogaps in plasmonic nanostructures or enable the study of electron transport in single molecules. We envision the incorporation of π-conjugated systems prior to seeding, thus circumventing solution-based and random deposition of the molecule after nanogap fabrication, while potentially achieving better control of the molecular orientation in the gap.

EXPERIMENTAL SECTION

Materials. *AuNR Synthesis.* Cetyltrimethylammonium bromide (CTAB, 99%), sodium tetrahydridoborate ($NaBH_4$, 99%), and hydrogen tetrachloroaurate(III) trihydrate ($HAuCl_4$, 99.9%) were obtained from Aldrich Chemicals. Ascorbic acid was obtained from Merck. All reagents were used as received, and all glassware was thoroughly cleaned with a solution of sulfuric acid and potassium dichromate before use. Water was purified using a Millipore Milli-Q setup for

ultrapure water (18.2 MΩ·cm). Si_3N_4 TEM grids were purchased from SPI supplies.

Chip Fabrication. Chips for directed growth and electrical characterization of AuNRs are fabricated using standard electron beam lithography (JEOL JSM-6301F, 100 keV) on thermally oxidized silicon substrates or Si_3N_4 TEM grids. Metallic contacts were formed by e-beam evaporation of chromium (7 nm) and gold (30 nm with a 5 nm Cr sticking layer) on patterned chips and lift-off in acetone followed by rinsing in isopropyl alcohol and water and blow-drying with N_2.

Synthesis of Seeds and Gold Nanorods on Surfaces. The gold nanoparticle seeds were prepared as previously reported.[43] In brief, 250 μL of 0.01 M of aqueous $HAuCl_4$ was added to 10 mL of 0.1 M CTAB in water. The solution turned orange, indicating the formation of a $CTA^+-AuCl_4^-$ complex. To this solution was added 0.6 mL of 0.01 M ice-cold $NaBH_4$, inducing a change in color to a dark brown due to formation of 2−3 nm particle seeds. The solution was vigorously stirred for 1 min followed by aging for a minimum of 2 hours at 27 °C.

Next, a substrate (either bare Si/SiO_2 or prepatterned) was immersed into the seeding solution for 10 min at 27 °C followed by thorough washing in ultrapure water. Seeded substrates were placed in a growth solution for 1 h at 27 °C followed by thorough washing and drying with N_2. The growth solution consists of 9 mL of 0.1 M CTAB, 250 μL of 0.01 M $HAuCl_4$, and 50 μL of freshly prepared 0.01 M ascorbic acid.

Imaging. SEM imaging of the chips was performed on a JEOL JSM-6320F operated at 30 kV or on a Zeiss Supra 60 VP operated at 10 keV. For TEM imaging, the growth was performed on Si_3N_4 membrane TEM grids and examined using a Philips CM 20 running at 200 kV.

Electrical Measurements. All measurements were performed on a Keithley 4200-SCS probe station at ambient conditions. After nanorod growth, the chips were rinsed in deionized water at 27 °C for 2 min and blown dry with N_2 for 10 s. For nanogap measurements, the chips were annealed at 110 °C in a N_2 atmosphere. If the chip was coated with PMMA, an additional dip in acetone for 15 min, rinse with isopropyl alcohol, and blow-dry with nitrogen was introduced just after AuNR growth. Prior to electrical characterization, the chips are rinsed in acetone and isopropyl alcohol and dried with N_2.

Conflict of Interest: The authors declare no competing financial interest.

Acknowledgment. The work was supported by the European Community Seventh Framework Program (FP7/2007-2013) under the Grant Agreement No. 213609 "SINGLE", by The Danish−Chinese Center for Molecular Nanoelectronics funded by the Danish National Research Foundation, by Chalmers Materials and Nano Areas of advance, and by the Swedish Research Council.

Supporting Information Available: Additional SEM images of the presented experiments together with control experiments, TEM images of seeded chips, and AuNR statistics. This material is available free of charge *via* the Internet at http://pubs.acs.org.

REFERENCES AND NOTES

1. Li, T.; Hu, W.; Zhu, D. Nanogap Electrodes. *Adv. Mater.* **2010**, *22*, 286–300.
2. Song, H.; Reed, M. A.; Lee, T. Single Molecule Electronic Devices. *Adv. Mater.* **2011**, *23*, 1583–1608.
3. Mayor, M. Watching the Gap Close. *Angew. Chem., Int. Ed.* **2009**, *48*, 5583–5585.
4. Pelton, M.; Aizpurua, J.; Bryant, G. Metal-Nanoparticle Plasmonics. *Laser Photonics Rev.* **2008**, *2*, 136–159.
5. Moreland, J.; Ekin, J. W. Electron Tunneling Experiments Using Nb-Sn "Break" Junctions. *J. Appl. Phys.* **1985**, *58*, 3888.
6. Reed, M. A. Conductance of a Molecular Junction. *Science* **1997**, *278*, 252–254.
7. Kubatkin, S.; Danilov, A.; Hjort, M.; Cornil, J.; Brédas, J.-L.; Stuhr-Hansen, N.; Hedegård, P.; Bjørnholm, T. Single-electron Transistor of a Single Organic Molecule with Access to Several Redox States. *Nature* **2003**, *425*, 698–701.
8. Park, H.; Park, J.; Lim, A.; Anderson, E.; Alivisatos, A.; McEuen, P. Nanomechanical Oscillations in a Single-C60 Transistor. *Nature* **2000**, *407*, 57–60.
9. van der Zant, H. S. J.; Kervennic, Y.-V.; Poot, M.; O'Neill, K.; de Groot, Z.; Thijssen, J. M.; Heersche, H. B.; Stuhr-Hansen, N.; Bjørnholm, T.; Vanmaekelbergh, D.; *et al.* Molecular Three-terminal Devices: Fabrication and Measurements. *Faraday Discuss.* **2006**, *131*, 347.
10. Moth-Poulsen, K.; Bjørnholm, T. Molecular Electronics with Single Molecules in Solid-State Devices. *Nat. Nanotechnol.* **2009**, *4*, 551–556.
11. Jain, T.; Westerlund, F.; Johnson, E.; Moth-Poulsen, K.; Bjørnholm, T. Self-Assembled Nanogaps *via* Seed-Mediated Growth of End-to-End Linked Gold Nanorods. *ACS Nano* **2009**, *3*, 828–834.
12. Tang, Q.; Tong, Y.; Jain, T.; Hassenkam, T.; Wan, Q.; Moth-Poulsen, K.; Bjørnholm, T. Self-Assembled Nanogaps for Molecular Electronics. *Nanotechnology* **2009**, *20*, 245205.
13. Petersen, A. B.; Thyrhaug, E.; Jain, T.; Kilsaa, K.; Bols, M.; Moth-Poulsen, K.; Harrit, N.; Bjørnholm, T. First Step in Chemical Preparation of Metal Nanogaps Bridged by Thiol End-Capped Molecular Wires. *J. Phys. Chem. B* **2010**, *114*, 11771–11777.
14. Chen, X.; Braunschweig, A. B.; Wiester, M. J.; Yeganeh, S.; Ratner, M. A.; Mirkin, C. A. Spectroscopic Tracking of Molecular Transport Junctions Generated by Using Click Chemistry. *Angew. Chem., Int. Ed.* **2009**, *48*, 5178–5181.
15. Dadosh, T.; Gordin, Y.; Krahne, R.; Khivrich, I.; Mahalu, D.; Frydman, V.; Sperling, J.; Yacoby, A.; Bar-Joseph, I. Measurement of the Conductance of Single Conjugated Molecules. *Nature* **2005**, *436*, 677–680.
16. Tsivion, D.; Schvartzman, M.; Popovitz-Biro, R.; von Huth, P.; Joselevich, E. Guided Growth of Millimeter-Long Horizontal Nanowires with Controlled Orientations. *Science* **2011**, *333*, 1003–1007.
17. Kundu, P.; Chandni, U.; Ghosh, A.; Ravishankar, N. Pristine, Adherent Ultrathin Gold Nanowires on Substrates and between Pre-defined Contacts *via* a Wet Chemical Route. *Nanoscale* **2012**, *4*, 433–437.
18. Green, J. E.; Choi, J. W.; Boukai, A.; Bunimovich, Y.; Johnston-Halperin, E.; Delonno, E.; Luo, Y.; Sheriff, B. A.; Xu, K.; Shin, Y. S.; *et al.* A 160-kilobit Molecular Electronic Memory Patterned at 10(11) Bits Per Square Centimetre. *Nature* **2007**, *445*, 414–417.
19. Caswell, K. K.; Wilson, J. N.; Bunz, U. H. F.; Murphy, C. J. Preferential End-to-End Assembly of Gold Nanorods by Biotin-Streptavidin Connectors. *J. Am. Chem. Soc.* **2003**, *125*, 13914–13915.
20. Shibu Joseph, S. T.; Ipe, B. I.; Pramod, P.; Thomas, K. G. Gold Nanorods to Nanochains: Mechanistic Investigations on Their Longitudinal Assembly Using α,ω-Alkanedithiols and Interplasmon Coupling. *J. Phys. Chem. B* **2006**, *110*, 150–157.
21. Sreeprasad, T. S.; Samal, A. K.; Pradeep, T. One-, Two-, and Three-Dimensional Superstructures of Gold Nanorods Induced by Dimercaptosuccinic Acid. *Langmuir* **2008**, *24*, 4589–4599.
22. Guerrero-Martínez, A.; Pérez-Juste, J.; Carbó-Argibay, E.; Tardajos, G.; Liz-Marzán, L. M. Gemini-Surfactant-Directed Self-Assembly of Monodisperse Gold Nanorods into Standing Superlattices. *Angew. Chem., Int. Ed.* **2009**, *48*, 9484–9488.
23. Ahmed, W.; Kooij, E. S.; van Silfhout, A.; Poelsema, B. Quantitative Analysis of Gold Nanorod Alignment after Electric Field-Assisted Deposition. *Nano Lett.* **2009**, *9*, 3786–3794.
24. Correa-Duarte, M. A.; Pérez-Juste, J.; Sánchez-Iglesias, A.; Giersig, M.; Liz-Marzán, L. M. Aligning Au Nanorods by Using Carbon Nanotubes as Templates. *Angew. Chem., Int. Ed.* **2005**, *44*, 4375–4378.
25. Murphy, C. J.; Orendorff, C. J. Alignment of Gold Nanorods in Polymer Composites and on Polymer Surfaces. *Adv. Mater.* **2005**, *17*, 2173–2177.
26. Pérez-Juste, J.; Rodríguez-González, B.; Mulvaney, P.; Liz-Marzán, L. M. Optical Control and Patterning of

Gold-Nanorod-Poly(vinyl alcohol) Nanocomposite Films. *Adv. Funct. Mater.* **2005**, *15*, 1065–1071.
27. Kuemin, C.; Stutz, R.; Spencer, N. D.; Wolf, H. Precise Placement of Gold Nanorods by Capillary Assembly. *Langmuir* **2011**, *27*, 6305–6310.
28. Holzner, F.; Kuemin, C.; Paul, P.; Hedrick, J. L.; Wolf, H.; Spencer, N. D.; Duerig, U.; Knoll, A. W. Directed Placement of Gold Nanorods Using a Removable Template for Guided Assembly. *Nano Lett.* **2011**, *11*, 3957–3962.
29. Lim, J. K.; Lee, B. Y.; Pedano, M. L.; Senesi, A. J.; Jang, J.-W.; Shim, W.; Hong, S.; Mirkin, C. A. Alignment Strategies for the Assembly of Nanowires with Submicron Diameters. *Small* **2010**, *6*, 1736–1740.
30. Huang, Y.; Duan, X.; Wei, Q.; Lieber, C. M. Directed Assembly of One-Dimensional Nanostructures into Functional Networks. *Science* **2001**, *291*, 630–633.
31. Joselevich, E.; Lieber, C. M. Vectorial Growth of Metallic and Semiconducting Single-Wall Carbon Nanotubes. *Nano Lett.* **2002**, *2*, 1137–1141.
32. Kang, S. J.; Kocabas, C.; Ozel, T.; Shim, M.; Pimparkar, N.; Alam, M. A.; Rotkin, S. V.; Rogers, J. A. High-Performance Electronics Using Dense, Perfectly Aligned Arrays of Single-Walled Carbon Nanotubes. *Nat. Nanotechnol.* **2007**, *2*, 230–236.
33. Jana, N. R.; Gearheart, L.; Murphy, C. J. Wet Chemical Synthesis of High Aspect Ratio Cylindrical Gold Nanorods. *J. Phys. Chem. B* **2001**, *105*, 4065–4067.
34. Taub, N.; Krichevski, O.; Markovich, G. Growth of Gold Nanorods on Surfaces. *J. Phys. Chem. B* **2003**, *107*, 11579–11582.
35. Wei, Z.; Mieszawska, A. J.; Zamborini, F. P. Synthesis and Manipulation of High Aspect Ratio Gold Nanorods Grown Directly on Surfaces. *Langmuir* **2004**, *20*, 4322–4326.
36. Wei, Z.; Zamborini, F. P. Directly Monitoring the Growth of Gold Nanoparticle Seeds into Gold Nanorods. *Langmuir* **2004**, *20*, 11301–11304.
37. Mieszawska, A. J.; Zamborini, F. P. Gold Nanorods Grown Directly on Surfaces from Microscale Patterns of Gold Seeds. *Chem. Mater.* **2005**, *17*, 3415–3420.
38. Mieszawska, A. J.; Slawinski, G. W.; Zamborini, F. P. Directing the Growth of Highly Aligned Gold Nanorods through a Surface Chemical Amidation Reaction. *J. Am. Chem. Soc.* **2006**, *128*, 5622–5623.
39. Murphy, C. J.; Thompson, L. B.; Chernak, D. J.; Yang, J. A.; Sivapalan, S. T.; Boulos, S. P.; Huang, J.; Alkilany, A. M.; Sisco, P. N. Gold Nanorod Crystal Growth: From Seed-Mediated Synthesis to Nanoscale Sculpting. *Curr. Opin. Colloid Interface Sci.* **2011**, *16*, 128–134.
40. Sharma, V.; Park, K.; Srinivasarao, M. Shape Separation of Gold Nanorods Using Centrifugation. *Proc. Natl. Acad. Sci. U.S.A.* **2009**, *106*, 4981–4985.
41. Liu, S.; Tok, J. B.-H.; Locklin, J.; Bao, Z. Assembly and Alignment of Metallic Nanorods on Surfaces with Patterned Wettability. *Small* **2006**, *2*, 1448–1453.
42. Krans, J. M.; Ruitenbeek, J. M.; van; Fisun, V. V.; Yanson, I. K.; de Jongh, L. J. The Signature of Conductance Quantization in Metallic Point Contacts. *Nature* **1995**, *375*, 767–769.
43. Nikoobakht, B.; El-Sayed, M. A. Preparation and Growth Mechanism of Gold Nanorods (NRs) Using Seed-Mediated Growth Method. *Chem. Mater.* **2003**, *15*, 1957–1962.